

# Efficient Fault Feature Extraction and Fault Isolation for High Voltage DC Transmissions

Zhixiong Li<sup>1,2</sup>, Chenxing Sheng<sup>3</sup>, Yuanjing Li<sup>4</sup>, Jingtang Xing<sup>5</sup>, Benyu Su<sup>1</sup>

<sup>1</sup>*School of Mechatronic Engineering & Jiangsu Key Laboratory of Mine Mechanical and Electrical Equipment, China University of Mining and Technology, University Road 1, 221116 Xuzhou, P. R. China*

<sup>2</sup>*School of Mechanical & Manufacturing Engineering, University of New South Wales, NSW 2052 Sydney, Australia*

<sup>3</sup>*School of Power & Energy Engineering, Wuhan University of Technology, Heping Road 74, 430063 Wuhan, China*

<sup>4</sup>*School of Engineering and the Environment, University of Southampton, SO17 1BJ Southampton, United Kingdom*

<sup>5</sup>*South China University of Technology, Wushan Road 384, 510006 Guangzhou, P. R. China*  
schxing@yeah.net

**Abstract**—High Voltage DC Transmission (HVDC) plays vital role in transmission and supply of high quality electric energy. The condition monitoring and protection are crucial for the normal operation of the HVDC system. Unfortunately, it is difficult to extract failure features and isolate the faults of HVDC because the transmission line always spreads a long distance. To address this issue, this work presents an efficient condition monitoring and fault diagnosis method for HVDC based on an independent component analysis (ICA)-wavelet feature extractor and a neural network fault classifier. The innovation of the proposed method lies that it appropriately introduced the ICA-wavelet to realize accurate fault feature extraction and the actual engineering data in Guangzhou HVDC system has been used to verify the effectiveness of the proposed method. The experimental results show that the new method can efficiently extract important fault features with heavy noise components depressed and the fault diagnosis rate reached to 83.3 %. Moreover, the proposed method is superior to the traditional methods. The findings of this work could provide valuable experience and data support for the construction and development of HVDC system in practice.

**Index Terms**—HVDC, fault detection, ICA, source separation.

## I. INTRODUCTION

Developed in Sweden and in Germany in 1930s and firstly applied commercially in Soviet Union in 1951, right now the high voltage direct current Transmission (HVDC) has been widely accepted as a new generation technology for the bulk transmission of electrical power [1]–[3]. Compared with the common alternating current (AC) systems, HVDC is more

economical in long-distance electrical power transmission [4]–[6]. For short distances, owing to excellent system performance in transient state and steady state, HVDC still warrants higher quality electrical power supply than AC systems [7]. Moreover, HVDC allows power flow running at different frequencies in two or more grid systems [8]. This feature will benefit incompatible networks in power transfer and improve the grid stability. Hence, HVDC lines have been now constructing extensively all over the world [9].

Although HVDC technology has achieved fast development, its protection theory is developing relatively slowly [10]. The main reasons limiting protection on HVDC are that the transmission line is very long and the fault mechanism is very complex [11]–[13]. Along with the rapid economic development of China and other countries, the electric power demand grows day by day; efficient and reliable power supply become very important. How to guarantee the performance of the HVDC transmission system, ensure system efficient, reliable, safe operation and timely discover and predict system fault, become a big challenge in HVDC systems [14], [15].

Recent progresses on the HVDC protection indicates that the time-frequency characteristics of the voltage and current of the HVDC components could provide significant information for HVDC fault detection and isolation [13], [16]–[18]. Liao *et al* [19] suggested in their research that the natural frequency of travelling wave of the HVDC is very useful for fault location. Xu and Huang [20] used the Wavelet to extract the time-frequency features of the HVDC fault diagnosis. Kerf *et al* [21] and Li *et al* [22] also proved that the Wavelet-based protection strategy is very suitable for HVDC fault detection and isolation. However, most of the existing work has not addressed the issue of separation of key signal source directly involved with the HVDC faults [23]. As well known, the HVDC line always spreads thousands of kilometres in distance. The voltage and current sensors have been serious contaminated by strong background noise and

Manuscript received April 11, 2015; accepted July 24, 2015.

This research was funded by the National Basic Research Program of China (973 Program) (No. 2014CB046300), the China Postdoctoral Science Foundation (No. 2014M551687), the Science Foundation of Jiangsu Province (No. BK20140200), the Fundamental Research Funds for the Central Universities (No. 2014QNA37), the State Foundation for Studying Abroad from China Scholarship Council (NO. 201406425014) and the Priority Academic Program Development of Jiangsu Higher Education Institutions.

disturbance signals. In the faults diagnosis procedure, only a small portion of source components in the sensor data is involved with the HVDC fault and could be sensitive for the changes of system conditions. The other background noise and disturbance signal components in the sensor data may greatly influence the fault detection and leads to false alarm and misdiagnosis [23]. If the key components useful for fault diagnosis could be separated from the sensor signal, the fault detection performance of Wavelet-based protection strategy will be improved. Unfortunately, very limited work has been done to address this issue. To solve this problem, we propose the independent component analysis (ICA) to separate useful fault source components from multi-channel sensor signals in the HVDC. The ICA is powerful to find a suitable representation of multi-channel sensor signals and has been proven to be very efficient to separate independent fault components from multi-channel sensors [24]. Hence, it is reasonable to evaluate the fault detection performance of Wavelet-based protection strategy after ICA processing.

Taking the HVDC system in Guangzhou city as the research object, this work presents a new early fault detection method of HVDC using ICA-Wavelet-based protection strategy. The mathematical model of HVDC system was firstly established to investigate the independent component analysis (ICA) based blind source separation technology to realize accurate fault signal extraction. Then, the inherent quantitative index of the fault characteristics was extracted using wavelet transform. Lastly, a neural network was employed to identify the HVDC faults. Both numerical simulation and actual engineering data in Guangzhou HVDC system have been used to verify the effectiveness of the proposed method. The analysis results show that the new method is promising in improving the potential failure detection and ensuring the HVDC operation efficiency and safety. The findings of this work can provide valuable experience and data support for the construction and development of HVDC system in Guangzhou.

## II. HVDC PROTECTION METHOD

Herein we firstly introduce the mathematical model of a typical two-terminal voltage source converter (VSC)-HVDC system. Based on the VSC-HVDC model the proposed fault detection method is described.

### A. VSC-HVDC Model

As shown in Fig. 1, the two-terminal VSC-HVDC system consists of two power sources, two VSC stations with DC capacitors and AC filters, DC transmission line, etc.

The two VSC stations are constructed symmetrically. The VSC at the AC side can be modeled in  $d$ - $q$  synchronous coordinates as [5]:

$$\begin{cases} L \frac{di_d}{dt} = -Ri_d + \tilde{S}Li_q + u_{sd} - u_{cd}, \\ L \frac{di_q}{dt} = -Ri_q - \tilde{S}Li_d + u_{sq} - u_{cq}, \\ C \frac{du_{dc}}{dt} = i_{dl} - i_{dc}, \end{cases} \quad (1)$$

where  $u_{sd,q}$  and  $i_{d,q}$  are the  $dq$  components of AC voltage

and current, respectively;  $u_{cd,q}$  are the  $dq$  components of VSC voltage;  $R$  and  $L$  are the VSC resistance and inductance, respectively;  $\tilde{S}$  is the AC frequency;  $u_{dc}$  and  $C$  are the DC bus voltage and DC capacitor, respectively;  $i_{dl}$  is the DC current to be filtered by  $C$  and  $i_{dc}$  is the DC bus current.

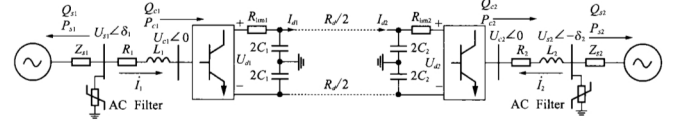


Fig. 1. Principle diagram of two-terminal HVDC.

Align the  $d$ -axis in phase with the AC source voltage, i.e.  $u_{sd} = u_s$ ,  $u_{sq} = 0$ , then the active and reactive power from the AC source to the DC link can be modeled as [7]:

$$\begin{cases} Q = -3u_{sd}i_q / 2, \\ P = 3u_{sd}i_d / 2, \end{cases} \quad (2)$$

where if  $u_{sd}$  is fixed, then  $Q$  is only proportional to  $i_q$ , and  $P$  is proportional to  $i_d$ . Therefore, the active and reactive power can be adjusted independently through direct control of  $i_q$  and  $i_d$ .

Based on this HVDC mathematical model, the development of the ICA-Wavelet based protection strategy has been proposed in this work.

### B. The Proposed Fault Detection Method

The HVDC system is very huge and complex. A measured voltage/current signal may be distorted due to strong background noise. In addition, the existing wavelet-based protection strategy only can process one sensor signal but it is difficult to determine the optimal sensor installation location. To solve these problems, this work presents a new method that uses ICA to fuse multi-channel sensor signals to find a suitable representation of fault characteristics [23]. By doing so, the wavelet-based protection strategy could be improved with respect to fault detection rate. The ICA is defined as

$$\mathbf{X} = \mathbf{A} \times \mathbf{S}, \quad (3)$$

where  $\mathbf{X} = [\mathbf{x}_1 \ \mathbf{x}_2 \ \cdots \ \mathbf{x}_p]^T$  is measured signals using  $p$  sensors;  $\mathbf{S} = [\mathbf{s}_1 \ \mathbf{s}_2 \ \cdots \ \mathbf{s}_q]^T$  is  $q$  unknown independent sources contained in the sensor data;  $\mathbf{A}$  is the mixing matrix. (3) indicates that for any sensor measurement  $\mathbf{x}_p$  there are  $q$  unknown independent sources hidden in the signal and among  $q$  sources there may be one or two sources are directly involved with the faults. One can note that if find the inverse matrix  $\mathbf{W}$  of  $\mathbf{A}$ , the  $q$  sources could be separated from  $\mathbf{X}$ , i.e.  $\hat{\mathbf{S}} = \mathbf{W} \cdot \mathbf{X} \approx \mathbf{S}$ . The negentropy iteration could be used to estimate  $\mathbf{W}$  [25]. The negentropy is defined as

$$J(\hat{\mathbf{S}}) \approx [E\{G(\hat{\mathbf{S}})\} - E\{G(\ )\}], \quad (4)$$

where  $E$  is the mathematical expectation,  $G$  is a non-quadratic function, and  $\hat{\mathbf{S}}$  is Gaussian variables with the

same covariance matrix of  $\hat{\mathbf{S}}$ . Hence, from (4) the ICA separation could be transferred into the following nonlinear optimal problem:

$$\begin{cases} \max_{\mathbf{W}} J(\hat{\mathbf{S}}), \\ \text{s.t. } E\{(W_i^T \mathbf{x})(W_j^T \mathbf{x})\} = \begin{cases} 1 & i=j, \\ 0 & i \neq j, \end{cases} \end{cases} \quad (5)$$

where  $\hat{\mathbf{S}} = [W_1 \mathbf{x} \ W_2 \mathbf{x} \ \dots \ W_q \mathbf{x}]^T$ . Then, apply the Kuhn-Tucker term and the fixed-point iteration to (5), to yield the updating of  $\mathbf{W}$ :

$$W^*(k+1) = E\{zg(W(k)^T z)\} - E\{g'(W(k)^T z)\}W(k), \quad (6)$$

$$W(k+1) = W^*(k+1) / \|W^*(k+1)\|, \quad (7)$$

where  $z$  is the whitening of  $\mathbf{X}$ , and  $g$  is the derivative function of  $G$ . Then de-mixing matrix  $W$  could be obtained by repeating (6) and (7) until the termination criterion is met.

After the ICA processing, useful fault sources have been extracted and are prepared for the Wavelet analysis. The Wavelet is a kind of time-frequency analysis technique. Wavelet can capture inherent features hidden in the signal by decomposing the signal into wavelet sub-bands divided equally in frequency along the time axis [21]. Since each wavelet sub-band presents a change of the original signal in a small piece of frequency band, the energy values of the wavelet sub-bands could be used as the fault feature vector. In this work the neural network has been employed to learn the relationship mapping the feature vector and the HVDC faults. Figure 2 shows the workflow diagram of the proposed fault diagnosis method.

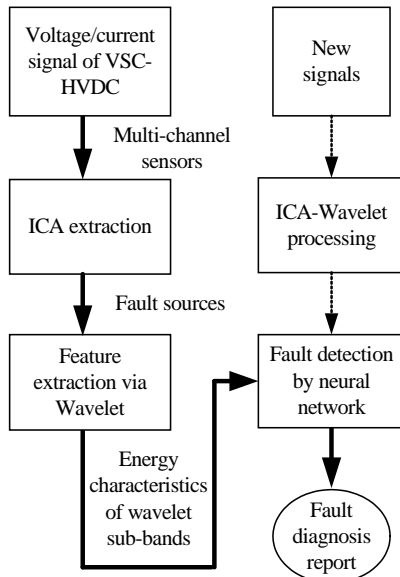


Fig. 2. The workflow diagram of the proposed fault diagnosis method.

### III. SIMULATION AND EXPERIMENT

#### A. Numerical Simulation and Discussion

A simulation model of the VSC-HVDC system shown in Fig. 1 has been established using MATLAB software. This model is strictly subjected to HVDC mathematical model.

The electrical power is transmitted by two VSC stations from a 110 kV, 50 Hz AC source to another identical one. The DC transmission line is 500 km.  $R = 0.01$ ,  $L = 0.05$  H,  $C = 0.001$  F. In order to measure the system DC voltage signals, 10 sensors have been installed along the DC line with an interval of 50 km.

In the simulation, 3 kinds of typical HVDC faults were introduced in the MATLAB model to investigate the fault detection performance of the proposed method. These faults include DC ground fault (DG), AC line-to-line fault (LL), and coupled fault of AC line-to-ground and line-to-line (LG-LL). Figure 3(a)–Fig. 3(d) shows the original system voltage signals under normal and faulty states and Fig. 4(a)–Fig. 4(d) gives the voltage signals after ICA processing.

It can be seen in Fig. 3(a)–Fig. 3(d) that the original DC voltage signals have been corrupted by background noise. It is difficult to extract useful information for purpose of accurate fault diagnosis. This is why the ICA has been introduced in the fault feature extraction in this work. One can note in Fig. 4(a)–Fig. 4(d) that after the ICA processing the background disturbance has been depressed effectively. Compared with the original signals, the extracted DC voltage signals could represent obvious changes when faults occur. Thus, useful fault sources have been extracted by ICA.

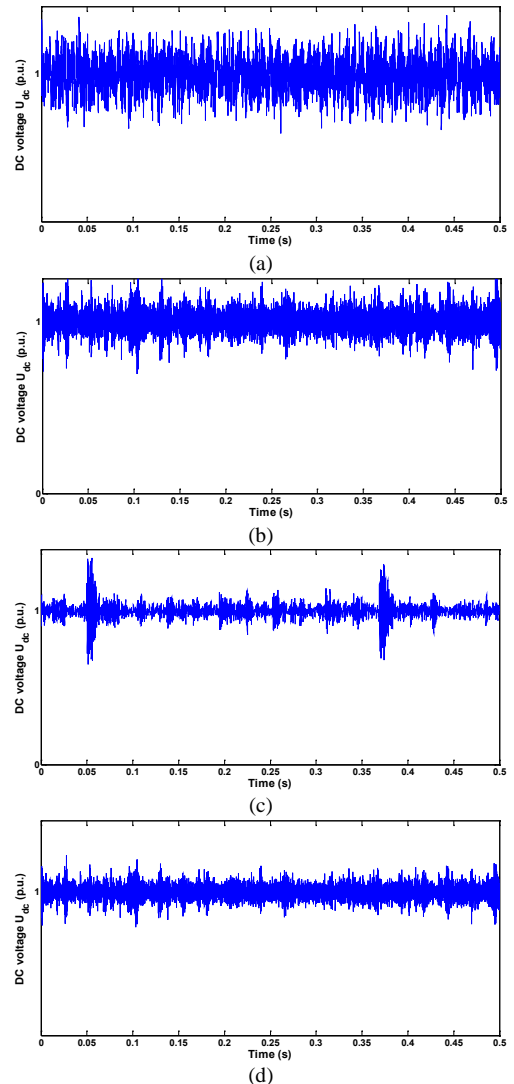


Fig. 3. The original DC voltage signals: (a) Normal state; (b) LL fault signal; (c) DG fault signal; (d) TLG-LL fault signal.

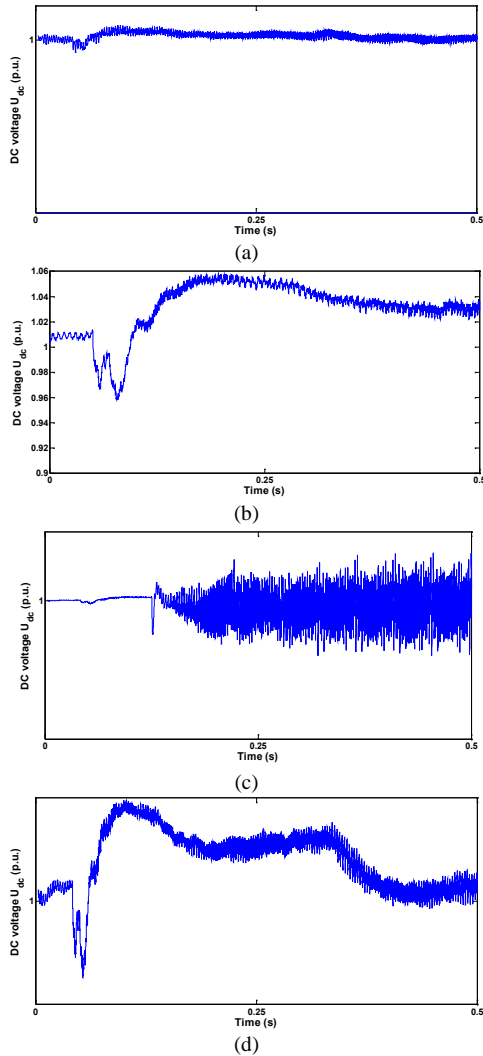


Fig. 4. The extracted DC voltage signals via ICA processing: (a) Normal state after ICA extraction; (b) LL fault signal after ICA extraction; (c) DG fault signal after ICA extraction; (d) TLG-LL fault signal after ICA extraction.

Then the Wavelet was used herein to decompose the extracted DC voltage signals in to 8 wavelet sub-bands. Table I–Table 4 show the energy distributions of the 8 wavelet sub-bands under the 4 system operation conditions. It

can be seen in the tables that the energy flow in the 8 sub-bands varies with the changes of the system conditions. For instance, in wavelet sub-band 1, its energy ratio accounted for 39 % of the whole signal energy under normal condition in Table I; however, when faults occurred the energy ratios changed to 27.1 % in Table II, 19.1 % in Table III and 30.5 % in Table IV, respectively. Hence, the energy values of the wavelet sub-bands could be used as the features for the fault identification.

TABLE I. ENERGY RATIO OF 8 WAVELET SUB-BANDS IN NORMAL STATE.

| Number of wavelet sub-bands |  |
|-----------------------------|--|
|                             | 1 2 3 4 5 6 7 8                                  |
| <b>Energy ratio</b>         | 39 % 25.7 % 7.7 % 13.8 % 2.3 % 4.1 % 3.5 % 3.9 % |

TABLE II. ENERGY RATIO OF 8 WAVELET SUB-BANDS IN LL STATE.

| Number of wavelet sub-bands |   |
|-----------------------------|---|
|                             | 1 2 3 4 5 6 7 8                                     |
| <b>Energy ratio</b>         | 27.1 % 20.8 % 12.6 % 21.6 % 2.5 % 4.1 % 5.7 % 5.6 % |

TABLE III. ENERGY RATIO OF 8 WAVELET SUB-BANDS IN DG STATE.

| Number of wavelet sub-bands |   |
|-----------------------------|---|
|                             | 1 2 3 4 5 6 7 8                                     |
| <b>Energy ratio</b>         | 19.1 % 25.6 % 17.8 % 22.8 % 1.7 % 3.3 % 8.5 % 5.2 % |

TABLE IV. ENERGY RATIO OF 8 WAVELET SUB-BANDS IN TLG-LL STATE.

| Number of wavelet sub-bands |  |
|-----------------------------|--|
|                             | 1 2 3 4 5 6 7 8                                    |
| <b>Energy ratio</b>         | 30.5 % 38.8 % 4.8 % 28.3 % 1.8 % 2.4 % 3.2 % 4.2 % |

TABLE VI. THE FAULT DETECTION RESULTS.

| Methods         | Detection rate (%) |
|-----------------|--------------------|
| Wavelet-NN      | 57.3%              |
| Wavelet-HMM     | 61.7%              |
| ICA-Wavelet-NN  | 83.3%              |
| ICA-Wavelet-HMM | 81.7%              |

TABLE V. A PORTION OF THE FAULT DETECTION RESULTS USING THE PROPOSED METHOD.

| Samples | Outputs of the neural network |              |              |              | Expected outputs | Detection results |
|---------|-------------------------------|--------------|--------------|--------------|------------------|-------------------|
|         | Neuron 1                      | Neuron 2     | Neuron 3     | Neuron 4     |                  |                   |
| 1       | 0.088                         | 0.071        | 0.024        | <b>0.954</b> | 0001             | Normal            |
| 2       | 0.195                         | 0.027        | 0.234        | <b>1.040</b> | 0001             | Normal            |
| 3       | 0.055                         | 0.031        | 0.041        | <b>0.932</b> | 0001             | Normal            |
| 4       | 0.149                         | 0.054        | 0.053        | <b>0.893</b> | 0001             | Normal            |
| 5       | 0.190                         | 0.035        | 0.111        | <b>1.061</b> | 0001             | Normal            |
| 6       | 0.062                         | 0.010        | <b>1.054</b> | 0.023        | 0010             | LL                |
| 7       | 0.130                         | 0.024        | <b>1.108</b> | 0.032        | 0010             | LL                |
| 8       | 0.184                         | 0.009        | <b>1.020</b> | 0.024        | 0010             | LL                |
| 9       | 0.035                         | 0.064        | <b>0.920</b> | 0.016        | 0010             | LL                |
| 10      | 0.087                         | 0.019        | <b>1.027</b> | 0.031        | 0010             | LL                |
| 11      | 0.018                         | <b>0.983</b> | 0.016        | 0.027        | 0100             | DG                |
| 12      | 0.030                         | <b>0.967</b> | 0.099        | 0.099        | 0100             | DG                |
| 13      | 0.044                         | <b>1.080</b> | 0.038        | 0.038        | 0100             | DG                |
| 14      | 0.089                         | <b>0.985</b> | 0.057        | 0.071        | 0100             | DG                |
| 15      | 0.070                         | <b>1.037</b> | 0.183        | 0.018        | 0100             | DG                |
| 16      | <b>1.080</b>                  | 0.008        | 0.004        | 0.008        | 1000             | TLG-LL            |
| 17      | <b>0.930</b>                  | 0.015        | 0.073        | 0.027        | 1000             | TLG-LL            |
| 18      | <b>0.931</b>                  | 0.097        | 0.095        | 0.016        | 1000             | TLG-LL            |
| 19      | <b>1.000</b>                  | 0.046        | 0.391        | 0.038        | 1000             | TLG-LL            |
| 20      | <b>1.081</b>                  | 0.036        | 0.131        | 0.360        | 1000             | TLG-LL            |

In this work, 300 samples for each HVDC condition were prepared to evaluate the fault detection performance. We calculated 8 energy values for each sample in the Wavelet analysis to form the feature vector. A neural network with the structure of  $8 \times 40 \times 4$  was established to identify the faults. The binary code was adopted in the outputs of the neural network to map the input features to the 4 HVDC states, i.e. [0 0 0 1], [0 0 1 0], [0 1 0 0] and [1 0 0 0] corresponding to normal, LL, DG and TLG-LL states, respectively. Half of the samples were used to train the network and the other half were used for testing. A portion of the fault detection results are listed in Table V. It can be seen in the table that the proposed fault detection method can efficiently identify the HVDC faults.

In order to highlight the proposed HVDC fault diagnosis method, we have compared the new ICA-Wavelet based protection strategy with some common used methods. Table VI shows the comparison results between the proposed method and the Hidden Markov Model (HMM) [26] based methods. One can be noticed from the table that (a) the ICA processing can efficiently prove the fault detection rate owing to its reliable feature extraction ability, and (b) the proposed ICA-Wavelet-NN method is better than the ICA-Wavelet-HMM.

### B. Experimental Results and Discussion

In order to further evaluate the performance of the newly proposed HVDC fault diagnosis method in practice, experiments using real data in Guangzhou 110 kV transmission lines have been carried out in this work. This 110 kV HVDC transmission line happened a serious DC ground fault in 2010. The DC voltage failure data has been recorded in the database of Guangzhou HVDC system. The failure data from 5 sensors was selected to investigate the fault diagnosis performance of the proposed method.

Figure 5 shows the original DC source and Fig. 6 gives the ICA extracted one. Comparing the two figures one can note that the fault independent source involved with the system failure has been perfectly separated from the original sensor signals.

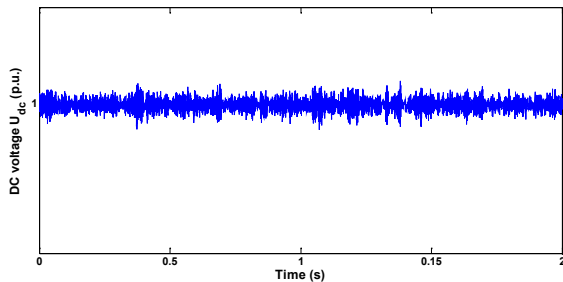


Fig. 5. The original DC voltage signal in Guangzhou 110 kV HVDC.

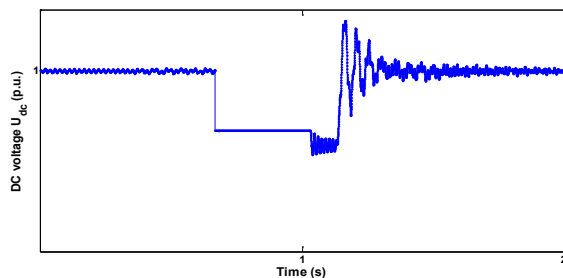


Fig. 6. The extracted DC voltage signal via ICA processing.

Then the ICA extracted DC voltage signals were decomposed by Wavelet analysis. Table VII and Table VIII show the energy distributions of the 8 wavelet sub-bands under normal and faulty conditions, respectively. Similar to Table I–Table IV, in Table VII and Table VIII the energy ratios of the sub-bands varied significantly with the change of the system health condition.

TABLE VII. ENERGY RATIO OF 8 WAVELET SUB-BANDS IN NORMAL STATE.

| Energy ratio | Number of wavelet sub-bands |        |        |       |        |        |        |        |
|--------------|-----------------------------|--------|--------|-------|--------|--------|--------|--------|
|              | 1                           | 2      | 3      | 4     | 5      | 6      | 7      | 8      |
|              | 24.3 %                      | 12.4 % | 18.6 % | 9.6 % | 10.3 % | 15.9 % | 10.7 % | 21.0 % |

TABLE VIII. ENERGY RATIO OF 8 WAVELET SUB-BANDS IN FAULTY STATE.

| Energy ratio | Number of wavelet sub-bands |        |       |        |       |       |       |       |
|--------------|-----------------------------|--------|-------|--------|-------|-------|-------|-------|
|              | 1                           | 2      | 3     | 4      | 5     | 6     | 7     | 8     |
|              | 23.6 %                      | 35.0 % | 7.5 % | 21.4 % | 1.7 % | 4.5 % | 2.8 % | 4.0 % |

Lastly, a neural network with the structure of  $8 \times 20 \times 3$  was established for the fault isolation. The binary code was adopted in the outputs, i.e. [0 0 1] and [1 0 0] corresponding to normal and DG states, respectively. We have extracted 50 samples of the normal state and 50 samples of the faulty state from the database of Guangzhou HVDC system. Thirty samples were used to train the network and the reminder 20 samples were used for testing. A portion of the fault detection results are listed in Table IX. It can be seen in the table that the proposed fault detection method can efficiently identify the HVDC faults.

TABLE IX. A PORTION OF THE FAULT DETECTION RESULTS.

| Samples | Outputs of the neural network |          |              | Expected outputs | Detection results |
|---------|-------------------------------|----------|--------------|------------------|-------------------|
|         | Neuron 1                      | Neuron 2 | Neuron 3     |                  |                   |
| 1       | 0.049                         | 0.182    | <b>1.063</b> | 001              | Normal            |
| 2       | -0.005                        | 0.008    | <b>1.081</b> | 001              | Normal            |
| 3       | 0.020                         | 0.138    | <b>1.102</b> | 001              | Normal            |
| 4       | -0.010                        | 0.082    | <b>1.072</b> | 001              | Normal            |
| 5       | 0.015                         | 0.079    | <b>0.946</b> | 001              | Normal            |
| 6       | <b>1.042</b>                  | 0.092    | 0.000        | 100              | DG                |
| 7       | <b>1.053</b>                  | 0.059    | 0.053        | 100              | DG                |
| 8       | <b>1.046</b>                  | 0.016    | 0.020        | 100              | DG                |
| 9       | <b>1.074</b>                  | 0.021    | 0.095        | 100              | DG                |
| 10      | <b>0.767</b>                  | 0.081    | 0.445        | 100              | DG                |

Table X compares the fault detection performance of the proposed method against the Hidden Markov Model (HMM) [26] based methods. It can be seen in the table that after the ICA processing both the Wavelet-NN and the Wavelet-HMM have dramatically improved the fault detection rate with a lift of 21.0 % or better. One can also note that the ICA-Wavelet-NN method is superior to the ICA-Wavelet-HMM with a 5.0 % improvement of detection rate.

TABLE X. THE FAULT DETECTION RESULTS.

| Methods         | Detection rate (%) |
|-----------------|--------------------|
| Wavelet-NN      | 57.5 %             |
| Wavelet-HMM     | 51.0 %             |
| ICA-Wavelet-NN  | 78.5 %             |
| ICA-Wavelet-HMM | 73.5 %             |

## IV. CONCLUSIONS

Taking the strong background disturbance mixed into the

sensor measurements into account, this work has reported the new feature extraction and fault isolation strategy for HVDC systems. The main innovation of the method is that the ICA feature extraction has been introduced into the existing Wavelet-based protection strategy to form the ICA-Wavelet based protection strategy. Both numerical simulation and experimental tests using real data have been implemented to illustrate the effectiveness of the proposed HVDC fault diagnosis method. The findings of the work suggest that the proposed ICA-Wavelet based protection strategy is reliable and feasible for fault diagnosis of HVDC systems and thus has practical importance. Future work will continue develop a remote condition monitoring and fault diagnosis system based on the ICA-Wavelet based protection strategy for the practical application of HVDC system protection.

## REFERENCES

- [1] C. Franck, "HVDC circuit breakers: A review identifying future research needs", *IEEE Trans. Power Delivery*, vol. 26, no. 2, pp. 998–1007, 2011. [Online]. Available: <http://dx.doi.org/10.1109/TPWRD.2010.2095889>
- [2] L. Chetty, N. Ijumba, "Quantitative feedback theory design of line current commutated HVDC control systems", *SAIEE Africa Research Journal*, vol. 104, no. 1, pp. 2–10, 2013.
- [3] X. Cui, X. Zhou, T. Lu, "Recent progress in the calculation methods of ion flow field of HVDC transmission lines", in *Proc. Chinese Society of Electrical Engineering*, vol. 32, no. 36, pp. 130–141, 2012.
- [4] U. Gnanarathna, A. Gole, R. Jayasinghe, "Efficient modeling of modular multilevel HVDC converters (MMC) on electromagnetic transient simulation programs", *IEEE Trans. Power Delivery*, vol. 26, no. 1, pp. 316–324, 2011. [Online]. Available: <http://dx.doi.org/10.1109/TPWRD.2010.2060737>
- [5] H. Ding, Y. Zhang, A. Gole, D. Woodford, M. Han, X. Xiao, "Analysis of coupling effects on overhead VSC-HVDC transmission lines from AC lines with shared right of way", *IEEE Trans. Power Delivery*, vol. 25, no. 4, pp. 2976–2986, 2010. [Online]. Available: <http://dx.doi.org/10.1109/TPWRD.2010.2043373>
- [6] S. Cole, B. Haut, "Robust modeling against model-solver interactions for high-fidelity simulation of VSC HVDC systems in EUROSTAG", *IEEE Trans. Power Systems*, vol. 28, no. 3, pp. 2632–2638, 2013. [Online]. Available: <http://dx.doi.org/10.1109/TPWRS.2012.2230194>
- [7] L. Wan, H. Ding, W. Liu, "Simulation model of control system for HVDC power transmission based on actual project", *Power System Technology*, vol. 37, no. 3, pp. 629–634, 2013.
- [8] P. Shao, L. Luo, Y. Li, C. Rehtanz, "Electromagnetic vibration analysis of the winding of a new HVDC converter transformer", *IEEE Trans. Power Delivery*, vol. 27, no. 1, pp. 123–130, 2012. [Online]. Available: <http://dx.doi.org/10.1109/TPWRD.2011.2174164>
- [9] Y. Li, F. Liu, L. Luo, C. Rehtanz, Y. Cao, "Enhancement of commutation reliability of an HVDC inverter by means of an inductive filtering method", *IEEE Trans. Power Electronics*, vol. 28, no. 11, pp. 4917–4929, 2013. [Online]. Available: <http://dx.doi.org/10.1109/TPEL.2013.2238641>
- [10] B. Soledad, A. Salvador, B. Ramon, R. Johel, "Efficiency and fault ride-through performance of a diode-rectifier-and VSC-inverter-based HVDC link for offshore wind farms", *IEEE Trans. Industrial Electronics*, vol. 60, no. 6, pp. 2401–2409, 2013. [Online]. Available: <http://dx.doi.org/10.1109/TIE.2012.2222855>
- [11] H. Lee, G. Son, J. Yoo, J. Park, "Effect of a SFCL on commutation failure in a HVDC system", *IEEE Trans. Applied Superconductivity*, vol. 23, no. 3, 2013.
- [12] M. Hu, C. Fu, J. Wang, X. Li, H. Liu, "Analysis of a parallel four-terminal HVDC transmission system based on real time digital simulation", *Automation of Electric Power Systems*, vol. 37, no. 5, pp. 87–92, 2013.
- [13] L. Xing, Q. Chen, Z. Gao, "A new protection principle for HVDC transmission lines based on directions of fault components of voltage and current", *Automation of Electric Power Systems*, vol. 37, no. 6, pp. 107–113, 2013.
- [14] Y. Liu, X. Li, Z. Cai, "Location of HVDC converter grounding fault", *Automation of Electric Power Systems*, vol. 34, no. 8, pp. 86–91, 2010.
- [15] H. Livani, C. Evrenosoglu, "A single-ended fault location method for segmented HVDC transmission line", *Electric Power Systems Research*, vol. 107, pp. 190–198, 2014. [Online]. Available: <http://dx.doi.org/10.1016/j.epsr.2013.10.006>
- [16] J. Suonan, J. Zhang, L. Yang, N. Wang, Y. Ma, "Distance protection for HVDC transmission line considering frequency-dependent parameters", *Automation of Electric Power Systems*, vol. 36, no. 16, pp. 63–69, 2012.
- [17] H. Shu, X. Tian, J. Dong, N. An, "Recognition method of HVDC transmission line fault based on multifractal spectrum", *Trans. of China Electrotechnical Society*, vol. 28, no. 1, pp. 251–258, 2013.
- [18] S. Gao, J. Suonan, G. Song, J. Zhang, Z. Hou, "A new pilot protection principle for HVDC transmission lines based on current fault component", *Automation of Electric Power Systems*, vol. 35, no. 5, pp. 52–56, 2010.
- [19] K. Liao, Z. He, X. Li, "Fault location of HVDC transmission line based on the natural frequency of traveling wave", *Automation of Electric Power Systems*, vol. 37, no. 3, pp. 104–109, 2013.
- [20] S. Xu, S. Huang, "Fault diagnosis of commutation failures in the HVDC system based on the wavelet energy spectrum and grey comprehensive relationship degree", *Power System Protection and Control*, vol. 40, no. 3, pp. 85–89, 2012.
- [21] K. Kerf, K. Srivastava, M. Reza, D. Bekaert, S. Cole, D. Hertem, R. Belmans, "Wavelet-based protection strategy for DC faults in multi-terminal VSC HVDC systems", *IET Generation, Transmission and Distribution*, vol. 5, no. 4, pp. 496–503, 2011. [Online]. Available: <http://dx.doi.org/10.1049/iet-gtd.2010.0587>
- [22] Z. Li, G. Lu, Y. Lv, "A novel scheme of HVDC transmission line voltage traveling wave protection based on wavelet transform", *Power System Protection and Control*, vol. 38, no. 13, pp. 40–45, 2010.
- [23] Z. Li, X. Yan, "Independent component analysis and manifold learning with applications to fault diagnosis of VSC-HVDC systems", *Hsi-An Chiao Tung Ta Hsueh*, vol. 45, no. 2, pp. 44–48, 2011.
- [24] Z. Li, X. Yan, Z. Guo, Y. Zhang, C. Yuan, Z. Peng, "Condition monitoring and fault diagnosis for marine diesel engines using information fusion techniques", *Elektronika Ir Elektrotechnika*, vol. 7, pp. 109–112, 2012. [Online]. Available: <http://dx.doi.org/10.5755/j01.eee.123.7.2387>
- [25] A. Hyvarinen, P. Hoyer, M. Inki, "Topographic independent component analysis", *Neural Computation*, vol. 7, pp. 1527–1558, 2001. [Online]. Available: <http://dx.doi.org/10.1162/089976601750264992>
- [26] M. Tahan, H. Monsef, S. Farhangi, "A new converter fault discrimination method for a 12-pulse high-voltage direct current system based on wavelet transform and Hidden Markov Models", *Simulation*, vol. 88, no. 6, pp. 668–679, 2012. [Online]. Available: <http://dx.doi.org/10.1177/0037549711413495>